SEMARAK ILMU PUBLISHING

Journal of Advanced Research in Fluid Mechanics and Thermal Sciences

Journal homepage:
https://semarakilmu.com.my/journals/index.php/fluid_mechanics_thermal_sciences/index
ISSN: 2289-7879

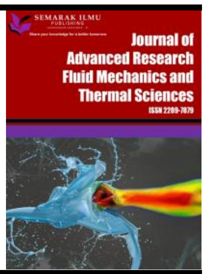

Time-Dependent MHD Free Convective Heat Circulation of Hybrid Nano Liquid over a Vertical Porous Plate Due to Temperature Oscillation with Thermal Radiation and Viscous Dissipation

S. V. Padma[1], M. P. Mallesh[1,*], Shankar Rao Munjam[2], Kottakkaran Sooppy Nisar[3]

[1] Department of Engineering Mathematics, Koneru Lakshmaiah Education Foundation Hyderabad Campus, Telangana, 50075, India
[2] School of Technology, Woxsen University, Hyderabad, Telangana-502345, India
[3] Department of Mathematics, College of Science and Humanities in Alkharj, Prince Sattam Bin Abdulaziz University, Alkharj 11942, Saudi Arabia

ARTICLE INFO

Article history:
Received 6 August 2023
Received in revised form 27 October 2023
Accepted 9 November 2023
Available online 30 November 2023

Keywords:
Free convection; MHD; hybrid nano liquid; temperature oscillation; viscous dissipation; thermal radiation

ABSTRACT

In the current numerical simulation, the thermal transfer of viscous incompressible time dependent MHD free convective flow of hybrid nanofluid (Cu-TiO_2-H_2O) over a vertical porous plate with viscous dissipation and thermal radiation is examined. The system of partial differential equations which controls the fluid flow are transmuted into dimensionless equations and are solved using numerical simulation namely Galerkin Finite Element Method. The momentum and thermal consequences, coefficient of heat transfer and skin friction with Gr, M, Ec, N, t, ωt, δ_2, λ – parameters for both nanofluid (Cu-H_2O) and hybrid nanofluid (Cu-TiO_2-H_2O) flows are exposed through graphs and tables. It is revealed that heat transfer coefficient of Cu-TiO_2-H_2O is more effective when compared with Cu-H_2O flows varying with aforementioned parameters. The current numerical computation is in good agreement with the analytical solution of the problem. This study is used in several engineering fields such as electronic cooling, heat exchangers, nanomaterial processing, environmental engineering, chemical industry.

1. Introduction

Transient MHD thermal convective circulations together with temperature oscillation in porous media is paramount in designing of natural and fluid engineering problems. Applications of MHD unsteady thermal convective circulations in nature and fluid engineering problems are of great technical importance in the areas such as geothermal energy extraction, MHD generators, elevation of thermal transfer in gas cooling systems, blood flow, accelerators, salinity difference in sea, cooling of nuclear power plants, electrical and electronic equipment etc. In view of aforesaid applications Vempati and Laxmi-Narayana-Gari [1] explored numerical simulation of natural convection and mass transmission on time dependent viscous liquid flow over an erect plane in presence of magnetism. Rashidi *et al.,* [2] analytically demonstrated mass and heat transformations on two-dimensional

* *Corresponding author.*
E-mail address: malleshmardanpally@gmail.com

https://doi.org/10.37934/arfmts.111.2.6585

hydromagnetic laminar flow with radiation over a porous surface. The buoyancy and heat transmission influence on hydromagnetic motion over a permeable surface is numerically examined by Daniel *et al.,* [3]. Singh *et al.,* [4] numerically described the heat transfer of free convective fluid flow past an infinite erect permeable surface with hydromagnetic influence. In view of aforesaid applications many scholars investigated MHD heat transformation fluid flow with various geometrical parameters [5-15]. The heat and mass transfer of MHD nanofluid flow with hall effects over different geometries is described by Singh *et al.,* [16,17]. The numerical study on MHD effects with viscous dissipation and chemical reaction of first order of heat and mass transfer over an upright stretching surface is investigated by Sharma and Gandhi [18]. Sharma *et al.,* [19] studied an incompressible fluid flow over an erect stretching surface to analyze heat and mass transfer impacts with ohmic heating, thermal and exponential heat source. Kumar *et al.,* [20] developed the sensitivity analysis of hybrid nano liquid over an up straight stretching surface with viscous dissipation, Joule heating impacts. Sharma *et al.,* [21] explored the influence of entropy generation, heat transmission, and mass transfer on the flow of Jeffrey fluid with solar radiation effect in the presence of copper nanoparticles and gyrotactic microorganisms. A numerical simulation to blood flow past a penetrable artery with an aneurysm under the electric and magnetic effect of hybrid nano liquid is scrutinized by Gandhi *et al.,* [22]. Reddy *et al.,* [23] numerically examined the impact the heat generation/absorption over a porous stretching cylinder on MHD thermal transfer flow of fluid.

Hybrid nano liquids are the next generation of nano liquids, which are acquired by scattering a homogeneous/non-homogeneous solution of composite nano powder of varied nanomaterials in a mixture of one or more base liquids. Hybridization of nanoparticles results a pristine physical and chemical bond which really make hybrid nano liquids to extend finer heat transfer performance than the conventional heat transmission and nano liquids with single nanoparticles. Hybrid nano liquids expanded their applications in every field like microelectronics, nuclear cooling, transportation, defence, naval structures, medical, drug delivery, pasteurization, solar energy conversion system, acoustics, liquid propulsion, heat transmission, manufacturing and so on. Vemula *et al.,* [24] explained numerical model of transient natural convection nano liquid flow of heat transmission past an erect surface. A comparative numerical flow and heat transfer analysis of nano liquid and Hybrid nano liquid over an enlarging sheet was performed by Devi and Devi [25,26]. The process of activation energy in thermo bioconvection nanofluid motion in a square cavity with gyrotactic microorganisms past a permeable surface is demonstrated by Bodduna *et al.,* [27]. Asogwa *et al.,* [28] numerically studied the heat generation with activation energy on hydrodynamic nanofluid flow over a stretching sheet. The usage of Hybrid nanofluids past a movable up right surface to amplify the free convective transmission of heat is numerically demonstrated by Rajesh *et al.,* [29]. Sharma *et al.,* [30] explored the effects of chemical reaction and thermal radiation of hybrid nanofluid flow over rotating disk. Mallesh *et al.,* [31] numerically scrutinized the heat generation and radiation effects on unsteady convective hybrid nanofluid flow over an upright oscillating plane.

Viscous dissipation is an irreversible phenomenon in which shear forces convert into heat due to the friction on flow between adjacent layers as a consequence mechanical energy is transmuted into heat energy. Viscous dissipation in Hybrid nano liquids acts an essential role in geophysical flows, aerodynamics and polymer processing. Reddy [32] numerically analyzed unsteady free convection flow on an upright sheet with viscous dissipation effect and magnetism. Zainal *et al.,* [33] demonstrated viscous dissipation impact on MHD stagnation flow over an expanding sheet in different nano liquids.

Thermal radiation has a major impact on thermal expansion in the boundary layer flow of a liquid at ambient temperature and is crucial in many technological applications including space technology, integrated circuit cooling, turbines, plasmas, missiles, satellites, design of space vehicles and aviation equipment. Bestman and Adjepong [34] analytically explored three-dimensional natural convection flow over a porous plane in a rotating motion. Makinde and Ogulu [35] numerically developed the influence of temperature-dependent viscosity with magnetism on natural convective laminar liquid flow over an up straight plane. Pal and Mondal [36] numerically scrutinized the radiation impact over a vertical sheet immersed in combined convective flows of optically thick viscous liquid. Jat and Chaudhary [37] numerically explored two-dimensional steady viscous fluid flow over a stretching sheet under the influence of Lorentz force and thermal radiation. Sandeep *et al.,* [38] and Chaudhary and Chaudhary [39] numerically demonstrated hydromagnetic and heat exchange properties on the different liquid flows over an exponentially stretching plane. Recently, numerical simulation of unsteady free convective CNT's nano liquid motion over an up straight plane with thermal variation is investigated by Kavitha *et al.,* [40].

Convective heat transfer in fluid-saturated porous media has received much attention since a decade due to its importance in various applications like nuclear waste repository, geothermal sciences, engineering, agriculture, combustion systems, heat pipes, enhanced oil reservoir recovery, thermal insulation engineering, hydro flow in geothermal reservoirs etc. Recently, numerous researchers have focused on radiative heat transfer and multiphase transport in porous medium, with and without phase change. Several researchers scrutinized heat transmission challenges in porous media on varied geometries [41-45]. Chaudhary *et al.,* [46] developed a numerical model on transient viscous liquid over a stretching surface using magnetic field and heat generation/absorption. Mixed convection two-dimensional steady flow pattern along permeable up right sheet with a hybrid nano liquid is numerically presented by Waini *et al.,* [47]. Sharma *et al.,* [48] studied the ternary hybrid nanofluid with blood as a host fluid for homogeneous and heterogeneous chemical reaction, thermal radiation, viscous dissipation effects over curved surfaces.

The heat transmission of incompressible time dependent MHD natural convective flow of hybrid nano liquid past a vertical permeable surface with thermal radiation and viscous dissipation and novel term temperature oscillation is described in this numerical simulation. The flow controlling equations of hybrid nanofluid in the form of partial differential equations are transformed into dimensionless equations employing similarity variables and are solved using a numerical approach namely Galerkin Finite Element Method. The graphical and tabular explanation is presented on momentum, thermal, heat transfer and skin friction coefficient with pertinent parameters of both Cu-H_2O and Cu-TiO_2-H_2O fluids. This numerical computation is in good agreement with the analytical solution of the problem. The current work has novel characteristics which are used in engineering fields such as nuclear coolants, heat exchangers, thermal image processing etc. The future scope of the present study is to explore the mixed convective flows over different geometries.

2. Flow Analysis and Solution

A laminar, incompressible time dependent MHD Cu-TiO_2-H_2O hybrid nano liquid flow over a vertical plate with viscous dissipation and thermal radiation effects are considered. We assumed a cartesian coordinate system (x^*, y^*) such that x^*- axis is taken vertically upwards along with the plate and y^*- axis is normal to the plate, which is presented in Figure 1. Initially, both the plate and fluid are kept steady and retained at free stream temperature $\theta^* = \theta^*_\infty$ for all $t' \leq 0$. When $t' > 0$, vertical plate commences being in motion with velocity $u_1^* = u_{1_0}^*$ and plate temperature is enhanced to $\theta^* = \theta^*_w + (\theta^*_w - \theta^*_\infty)\cos\omega^* t'$ and maintained uniform.

In the current study, Cu and TiO_2 nano particles with H_2O as base fluid is considered. Cu-H_2O is formed by scattering Cu nanoparticles of 0.1 volume fraction (δ_1= 0.1, is fixed throughout the simulation). To improve Cu-TiO_2-H_2O, titania nanoparticles with various volume fraction are dispersed in Cu-H_2O nanofluid. In the present scenario, Tiwari and Das [49] nano liquid model with Boussinesq approximation is considered [50]. The main assumption of Boussinesq approximation is that the density variations in the fluid can be neglected except in the buoyancy term of the Navier-stokes equations. The above assumptions are used to study the heat transfer characteristics of hybrid nano fluid flow in several engineering and bio-medical applications such as heat exchangers, polymer industries, drug delivery for chemo therapy processing etc. In view of these applications the frontier flow control equations of hybrid nano liquid are

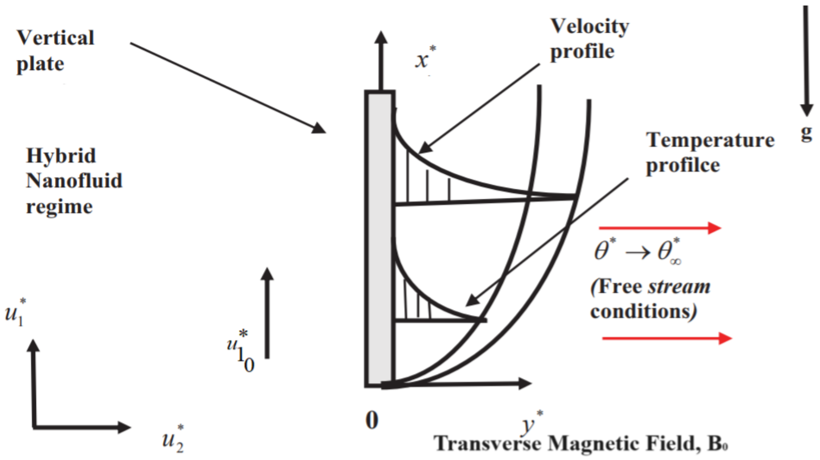

Fig. 1. Geometrical model

$$\frac{\partial u_2^*}{\partial y^*} = 0 \tag{1}$$

$$\rho_{hnf}\left[\frac{\partial u_1^*}{\partial t'} + u_2^*\frac{\partial u_1^*}{\partial y^*}\right] = \mu_{hnf}\frac{\partial^2 u_1^*}{\partial y^{*2}} + (\rho\beta)_{hnf}\, g\left(\theta^* - \theta^*_\infty\right) - \sigma_{hnf} B_0^2 u_1^* \tag{2}$$

$$\left(\rho C_p\right)_{hnf}\left[\frac{\partial \theta^*}{\partial t'} + u_2^*\frac{\partial \theta^*}{\partial y^*}\right] = \kappa_{hnf}\frac{\partial^2 \theta^*}{\partial y^{*2}} - \frac{\partial q_R^*}{\partial y^*} + \mu_{hnf}\left(\frac{\partial u_1^*}{\partial y^*}\right)^2 \tag{3}$$

Where,

$$q_R^* \text{ (radiative flux) } = -\frac{4\sigma_s}{3k_e}\frac{\partial \theta^{*4}}{\partial y^*} \tag{4}$$

Here σ_s represents absorption coefficient and K_e represents Stefan Boltzmann constant. The present study is assumed to optically thick nano liquids with Rosseland approximation. If temperature variations with in the stream are considered, then θ^{*4} can be represented as temperature lineal function using Taylor's series for θ^{*4} about θ^*_∞, and ignoring components of highest order we get,

$$\theta^{*4} \cong 4\theta_\infty^{*3}\theta^* - 3\theta_\infty^{*4} \tag{5}$$

Eq. (4) on differentiating, we obtain

$$\frac{\partial q_R^*}{\partial y^*} = -\frac{16\sigma_s\left(\theta_\infty^*\right)^3}{3k_e}\frac{\partial^2\theta^*}{\partial y^{*^2}} \tag{6}$$

Taken into consideration of Eq. (4), Eq. (5) and Eq. (6), Eq. (3) is simplified as,

$$\left(\rho C_p\right)_{hnf}\left[\frac{\partial\theta^*}{\partial t'} + u_2^*\frac{\partial\theta^*}{\partial y^*}\right] = \kappa_{hnf}\frac{\partial^2\theta^*}{\partial y^{*^2}} + \frac{16\sigma_s\left(\theta_\infty^*\right)^3}{3k_e}\frac{\partial^2\theta^*}{\partial y^{*^2}} + \mu_{hnf}\left(\frac{\partial u_1^*}{\partial y^*}\right)^2 \tag{7}$$

The ancillary constraints are

$$\begin{aligned}
&t' \le 0, \quad u_1^* = 0, \quad \theta^* = \theta_\infty^* && \text{for all} \quad y^* \\
&t' > 0, \quad u_1^* = u_{1_0}^*, \quad \theta^* = \theta_w^* + (\theta_w^* - \theta_\infty^*)\cos\omega^* t' && \text{at} \quad y^* = 0 \\
&\qquad\quad u_1^* \to 0, \quad \theta^* \to \theta_\infty^* && \text{as} \quad y \to \infty
\end{aligned} \tag{8}$$

Eq. (1) gives $u_2^* = -u_{2_0}^*\left(u_{2_0}^* > 0\right)$

Here, $u_{2_0}^*$ = constant suction velocity, and is towards the plate. Table 1 exhibits the Thermal features of water and nanoparticles. The necessary thermal parameters of Hybrid nano liquid ρ_{hnf}, μ_{hnf}, $\left(\rho C_p\right)_{hnf}$, $\left(\rho\beta\right)_{hnf}$, K_{hnf} are displayed in Table 2.

Table 1
Physical and Thermal physical attributes of water and nanoparticles [51]

	$\rho\left(kg/m^3\right)$	$C_p\left(J/kgK\right)$	$\kappa\left(W/mK\right)$	$\sigma\left(s/m\right)$	$\beta\left(1/K\right)$
H_2O	997.1	4179	0.613	5.5×10^{-6}	21×10^{-5}
Cu	8933	385	401	59.6×10^{6}	1.67×10^{-5}
TiO_2	4250	686.2	8.9528	2.6×10^{6}	0.9×10^{-5}

Table 2
Thermo physical attributes of nano liquid and hybrid nano liquid

Properties	Nano liquid $Cu-H_2O$	Hybrid Nano liquid $Cu-TiO_2-H_2O$
Density	$\rho_{nf}=\delta_1\rho_s+(1-\delta_1)\rho_f$	$\rho_{hnf}=\left\{(1-\delta_2)\left[(1-\delta_1)\rho_f+\delta_1\rho_{s1}\right]\right\}+\delta_2\rho_{s2}$
Heat Capacity	$(\rho C_p)_{nf}=\delta_1(\rho C_p)_s+(1-\delta_1)(\rho C_p)_f$	$(\rho C_p)_{hnf}=\left\{(1-\delta_2)\left[(1-\delta_1)(\rho C_p)_f+\delta_1(\rho C_p)_{s1}\right]\right\}+\delta_2(\rho C_p)_{s2}$
Viscosity	$\mu_{nf}=\dfrac{\mu_f}{(1-\delta_1)^{2.5}}$	$\mu_{hnf}=\dfrac{\mu_f}{(1-\delta_1)^{2.5}(1-\delta_2)^{2.5}}$
Thermal Conductivity	$\dfrac{\kappa_{nf}}{\kappa_f}=\dfrac{\kappa_s(n-1)\kappa_f-(n-1)\delta_1(\kappa_f-\kappa_s)}{\kappa_s+(n-1)\kappa_f+\delta_1(\kappa_f-\kappa_s)}$	$\kappa_{hnf}=\kappa_{bf}\left[\dfrac{\kappa_{s2}+(n_1-1)\kappa_{bf}-(n_1-1)\delta_2(\kappa_{bf}-\kappa_{s2})}{\kappa_{s2}+(n_1-1)\kappa_{bf}+\delta_2(\kappa_{bf}-\kappa_{s2})}\right]$ Where $\kappa_{bf}=\kappa_f\left[\dfrac{\kappa_{s1}+(n_1-1)\kappa_f-(n_1-1)\delta_1(\kappa_f-\kappa_{s1})}{\kappa_{s1}+(n_1-1)\kappa_f+\delta_1(\kappa_f-\kappa_{s1})}\right]$
Thermal Expansion Coefficient	$(\rho\beta)_{nf}=(1-\delta_1)(\rho\beta)_f+\delta_1(\rho\beta)_s$	$(\rho\beta)_{hnf}=(1-\delta_2)\left\{(1-\delta_1)(\rho\beta)_f+\delta_1(\rho\beta)_{s_1}\right\}+\delta_2(\rho\beta)_{s_2}$
Electrical Conductivity	$\sigma_{nf}=\sigma_f\left[\dfrac{\sigma_s(1+2\delta_1)+2\sigma_f(1-\delta_1)}{\sigma_s(1-\delta_1)+\sigma_f(2+\delta_1)}\right]$	$\sigma_{hnf}=\sigma_{bf}\left[\dfrac{\sigma_{s_2}(1+2\delta_2)+2\sigma_{bf}(1-\delta_2)}{\sigma_{s_2}(1-\delta_2)+\sigma_{bf}(2+\delta_2)}\right]$, Where $\sigma_{bf}=\sigma_f\left[\dfrac{\sigma_{s_1}(1+2\delta_1)+2\sigma_f(1-\delta_1)}{\sigma_{s_1}(1-\delta_1)+\sigma_f(2+\delta_1)}\right]$

Utilizing the relations,

$$u_1=\frac{u_1^*}{u_{1_0}^*},\ t=\frac{t'u_{1_0}^*}{\nu_f},\ y=\frac{y^*u_{1_0}^*}{\nu_f}=\frac{y^*}{L_{ref}}\ ,\ \theta=\frac{\theta^*-\theta_\infty^*}{\theta_w^*-\theta_\infty^*} \tag{9}$$

After non-dimensioning, the flow controlling equations are

$$\frac{\partial u_2}{\partial y}=0 \tag{10}$$

$$\frac{\partial u_1}{\partial t}-\lambda\frac{\partial u_1}{\partial y}=\frac{G_2}{G_1}\frac{\partial^2 u_1}{\partial y^2}+\frac{G_3}{G_1}Gr\theta-\frac{G_4}{G_1}Mu_1 \tag{11}$$

$$\frac{\partial\theta}{\partial t}-\lambda\frac{\partial\theta}{\partial y}=\left(G_6+\frac{4}{3N}\right)\frac{1}{G_5\,\mathrm{P}_r}\frac{\partial^2\theta}{\partial y^2}+\frac{G_2Ec}{G_5}\left(\frac{\partial u_1}{\partial y}\right)^2 \tag{12}$$

The analogous ancillary relations:

$$
\begin{aligned}
&t \le 0, \quad u_1 = 0, \quad \theta = 0 && \text{for all } y \\
&t > 0, \quad u_1 = 1, \quad \theta = 1 + \cos\omega t && \text{at } y = 0 \\
&\qquad\quad\; u_1 \to 0, \quad \theta \to 0 && \text{as } y \to \infty
\end{aligned}
\tag{13}
$$

Here,

$$
P_r = \frac{\nu_f}{\alpha_f} = \frac{(\mu C_p)_f}{k_f}, \quad \lambda = -\frac{u_2^*}{u_{1_0}^*}, \quad Gr = \frac{g\beta_f \nu_f (\theta_w^* - \theta_\infty^*)}{(u_{1_0}^*)^3},
$$

$$
M = \frac{\sigma_f B_0^2 \nu_f}{\rho_f u_{1_0}^2}, \quad N = \frac{k_f k_e}{4\sigma_s \theta_\infty^{*3}}, \quad Ec = \frac{u_{1_0}^{*2}}{(C_p)_f (\theta_w^* - \theta_\infty^*)}. \tag{14}
$$

where,

$$
\begin{aligned}
G_1 &= \left[(1-\delta_2)\left\{(1-\delta_1) + \delta_1 \frac{\rho_{s_1}}{\rho_f}\right\}\right] + \delta_2 \frac{\rho_{s_2}}{\rho_f}, \\
G_2 &= \frac{1}{(1-\delta_1)^{2.5}(1-\delta_2)^{2.5}}, \\
G_3 &= \left[(1-\delta_2)\left\{(1-\delta_1) + \delta_1 \frac{(\rho\beta)_{s_1}}{(\rho\beta)_f}\right\}\right] + \delta_2 \frac{(\rho\beta)_{s_2}}{(\rho\beta)_f}, \\
G_4 &= \frac{\sigma_{bf}}{\sigma_f}\left[\frac{\sigma_{s_2}(1+2\delta_2) + 2\sigma_{bf}(1-\delta_2)}{\sigma_{s_2}(1-\delta_2) + \sigma_{bf}(2+\delta_2)}\right], \\
G_5 &= \left[(1-\delta_2)\left\{(1-\delta_1) + \delta_1 \frac{(\rho C_p)_{s_1}}{(\rho C_p)_f}\right\}\right] + \delta_2 \frac{(\rho C_p)_{s_2}}{(\rho C_p)_f}, \\
G_6 &= \frac{\kappa_{bf}}{\kappa_f}\frac{\left[\kappa_{s_2} + (n_1-1)\kappa_{bf} - (n_1-1)\delta_2(\kappa_{bf} - \kappa_{s_2})\right]}{\left[\kappa_{s_2} + (n_1-1)\kappa_{bf} + \delta_2(\kappa_{bf} - \kappa_{s_2})\right]}.
\end{aligned}
\tag{15}
$$

The analytical solution of Eq. (12) without the convective and viscous dissipation terms subject to frontier constraints (13) when $\left(\omega t = \pi/2\right)$, using Laplace transform technique is obtained as:

$$
\theta = erfc\left(\frac{y\sqrt{pr}}{2\sqrt{\left(G_6 + \frac{4}{3N}\right)\frac{t}{G_5}}}\right) \tag{16}
$$

3. Surface Engineering Properties

In this work, two dispensable parameters of engineering relevance, namely Coefficient of skin friction (C_f) and the heat transfer (Nu), are computed numerically and given as

$$C_f = \frac{\tau_w}{\rho_f u_{1_0}^{*2}}, \quad Nu = \frac{q_w L_{ref}}{\kappa_f (\theta_w^* - \theta_\infty^*)} \tag{17}$$

Here τ_w designates Skin-friction or shear stress and q_w designates rate of heat transmission as

$$\tau_w = \mu_{hnf} \left(\frac{\partial u_1^*}{\partial y^*} \right)_{y^*=0}, \quad q_w = -\kappa_{hnf} \left(\frac{\partial \theta^*}{\partial y^*} \right)_{y^*=0} \tag{18}$$

Utilizing dimensionless components in (10), we attain

$$C_f = \frac{1}{(1-\delta_1)^{2.5}(1-\delta_2)^{2.5}} \left(\frac{\partial u_1}{\partial y} \right)_{y=0}, \; Nu = -\frac{\kappa_{hnf}}{\kappa_f} \left(\frac{\partial \theta}{\partial y} \right)_{y=0} \tag{19}$$

4. Solution Procedure

A robust Galerkin finite element approach, as shown in Figure 2, has decoded the PDE's (11) and (12) with inclusive pertinent conditions (13). The fundamental steps involved in this method are outlined by Rajesh and Chamkha [52], Reddy [53], and Bathe [54]. The analogous finite element equations on employing the Galerkin finite element procedure for Eq. (11) and Eq. (12) on the component (e) $\left(y_j \le y \le y_k \right)$ gives

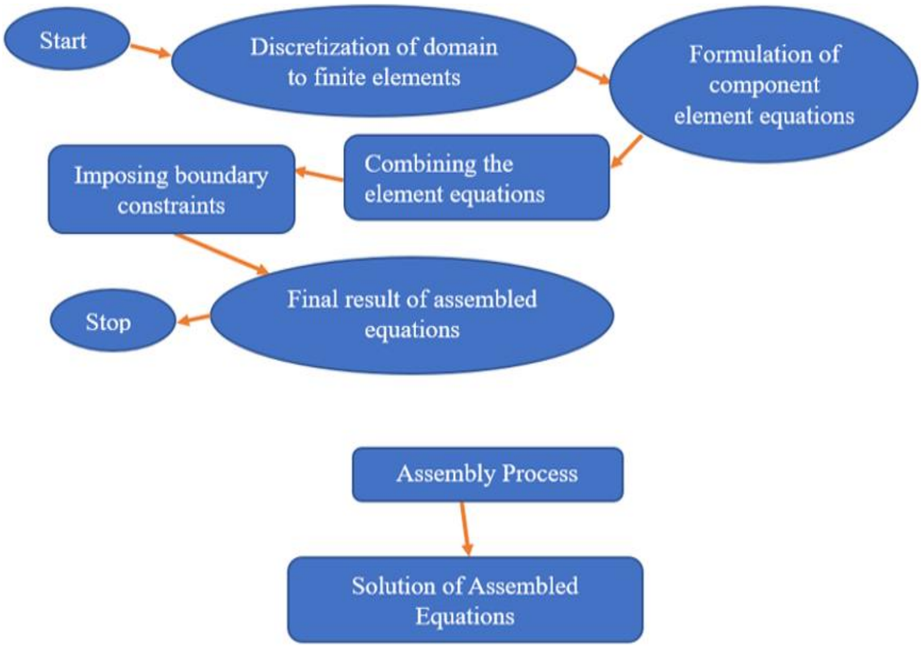

Fig. 2. Flow chart – Galerkin Finite Element Method [8]

$$\int_{y_j}^{y_k} N^{*(e)^{\theta}} \left(\frac{G_2}{G_1} \frac{\partial^2 u_1^{(e)}}{\partial y^2} + \lambda \frac{\partial u_1^{(e)}}{\partial y} - \frac{\partial u_1^{(e)}}{\partial t} + \frac{G_3}{G_1} Gr\theta - \frac{G_4}{G_1} M u_1 \right) dy = 0 \tag{20}$$

$$\int_{y_j}^{y_k} N^{*(e)^{\theta}} \left(\left[G_6 + \frac{4}{3N} \right] \frac{1}{P_r G_5} \frac{\partial^2 \theta^{(e)}}{\partial y^2} + \lambda \frac{\partial \theta^{(e)}}{\partial y} - \frac{\partial \theta^{(e)}}{\partial t} + \frac{G_2 E_c}{G_5} \left(\frac{\partial u_1}{\partial y} \right)^2 \right) dy = 0 \tag{21}$$

On integrating Eq. (20) on both sides with respect to y, we get

$$\begin{gathered} \left(\frac{G_2}{G_1} \right) \int_{y_j}^{y_k} N^{*(e)^{\theta}} \frac{\partial^2 u_1^{(e)}}{\partial y^2} dy + \lambda \int_{y_j}^{y_k} N^{*(e)^{\theta}} \frac{\partial u_1^{(e)}}{\partial y} dy - \int_{y_j}^{y_k} N^{*(e)^{\theta}} \frac{\partial u_1^{(e)}}{\partial t} dy + \\ \left(\frac{G_3}{G_1} \right) Gr\theta \int_{y_j}^{y_k} N^{*(e)^{\theta}} dy - \left(\frac{G_4}{G_1} \right) M \int_{y_j}^{y_k} N^{*(e)^{\theta}} u_1 dy = 0 \end{gathered} \tag{22}$$

Applying Integration by parts to Eq. (22),

$$\begin{gathered} \left(\frac{G_2}{G_1} \right) \left[N^{*(e)^{\theta}} \frac{\partial u_1^{(e)}}{\partial y} \right]_{y_j}^{y_k} - \left(\frac{G_2}{G_1} \right) \int_{y_j}^{y_k} \frac{\partial \left(N^{*(e)^{\theta}} \right)}{\partial y} \frac{\partial u_1^{(e)}}{\partial y} dy + \lambda \int_{y_j}^{y_k} N^{*(e)^{\theta}} \frac{\partial u_1^{(e)}}{\partial y} dy - \int_{y_j}^{y_k} N^{*(e)^{\theta}} \frac{\partial u_1^{(e)}}{\partial t} dy = \\ - \left(\frac{G_3}{G_1} \right) Gr\theta \int_{y_j}^{y_k} N^{*(e)^{\theta}} dy + \left(\frac{G_4}{G_1} \right) M \int_{y_j}^{y_k} N^{*(e)^{\theta}} u_1 dy \end{gathered} \tag{23}$$

Neglect the first term and multiply Eq. (23) by (-1) the simplified equation is

$$\begin{gathered} \left(\frac{G_2}{G_1} \right) \int_{y_j}^{y_k} \frac{\partial \left(N^{*(e)^{\theta}} \right)}{\partial y} \frac{\partial u_1^{(e)}}{\partial y} dy - \lambda \int_{y_j}^{y_k} N^{*(e)^{\theta}} \frac{\partial u_1^{(e)}}{\partial y} dy + \int_{y_j}^{y_k} N^{*(e)^{\theta}} \frac{\partial u_1^{(e)}}{\partial t} dy = \\ \left(\frac{G_3}{G_1} \right) Gr\theta \int_{y_j}^{y_k} N^{*(e)^{\theta}} dy - \left(\frac{G_4}{G_1} \right) M \int_{y_j}^{y_k} N^{*(e)^{\theta}} u_1 dy \end{gathered} \tag{24}$$

Consider the lineal piecewise approximation solution be

$$u_1^{(e)} = N_j^*(y) u_{1_j}(t) + N_k^*(y) u_{1_k}(t) = N_j^* u_{1_j} + N_k^* u_{1_k} \tag{25}$$

$$\theta^{(e)} = N_j^*(y) \theta_j(t) + N_k^*(y) \theta_k(t) = N_j^* \theta_j + N_k^* \theta_k \tag{26}$$

Where

$$N_j^* = \frac{y_k - y}{y_k - y_j},\ N_k^* = \frac{y - y_j}{y_k - y_j},\ N^{*(e)'} = \left[N_j^* \ N_k^* \right]' = \begin{bmatrix} N_j^* \\ N_k^* \end{bmatrix} \text{ are base functions.} \tag{27}$$

On simplifying, we get

$$\left(\frac{G_2}{G_1}\right)\int_{y_j}^{y_k}\begin{bmatrix} N_j^{*'}N_j^{*'} & N_j^{*'}N_k^{*'} \\ N_k^{*'}N_j^{*'} & N_k^{*'}N_k^{*'}\end{bmatrix}\begin{bmatrix} u_{1_j} \\ u_{1_k}\end{bmatrix}dy-\lambda\int_{y_j}^{y_k}\begin{bmatrix} N_j^{*(e)}N_j^{*(e)'} & N_j^{*(e)}N_k^{*(e)'} \\ N_k^{*(e)}N_j^{*(e)'} & N_k^{*(e)}N_k^{*(e)'}\end{bmatrix}\begin{bmatrix} u_{1_j} \\ u_{1_k}\end{bmatrix}dy+\int_{y_j}^{y_k}\begin{bmatrix} N_j^{*(e)}N_j^{*(e)} & N_j^{*(e)}N_k^{*(e)} \\ N_k^{*(e)}N_j^{*(e)} & N_k^{*(e)}N_k^{*(e)}\end{bmatrix}\begin{bmatrix} \dot{u}_{1_j} \\ \dot{u}_{1k}\end{bmatrix}dy = \left(\frac{G_3}{G_1}\right)Gr\,\theta\int_{y_j}^{y_k}\begin{bmatrix} N_j^{*(e)} \\ N_k^{*(e)}\end{bmatrix}dy-\left(\frac{G_4}{G_1}\right)M\int_{y_j}^{y_k}\begin{bmatrix} N_j^{*(e)}N_j^{*(e)} & N_j^{*(e)}N_k^{*(e)} \\ N_k^{*(e)}N_j^{*(e)} & N_k^{*(e)}N_k^{*(e)}\end{bmatrix}\begin{bmatrix} u_{1_j} \\ u_{1_k}\end{bmatrix}dy \tag{28}$$

Since, $u_1^{(e)} = N^{*(e)}\psi^{*(e)}$ then $\dfrac{\partial u_1^{(e)}}{\partial y} = \dfrac{\partial N^{*(e)}}{\partial y}\psi^{*(e)}$ and $\dfrac{\partial u_1^{(e)}}{\partial t} = N^{*(e)}\dfrac{\partial \psi^{*(e)}}{\partial y}$,

$y_k - y_j = l_e$ (Length of the element)

$$\left(\frac{G_2}{G_1 l_e}\right)\begin{bmatrix} 1 & -1 \\ -1 & 1\end{bmatrix}\begin{bmatrix} u_{1_j} \\ u_{1_k}\end{bmatrix}-\left(\frac{\lambda}{2}\right)\begin{bmatrix} -1 & 1 \\ -1 & 1\end{bmatrix}\begin{bmatrix} u_{1_j} \\ u_{1_k}\end{bmatrix}+\left(\frac{l_e}{6}\right)\begin{bmatrix} 2 & 1 \\ 1 & 2\end{bmatrix}\begin{bmatrix} \dot{u}_{1_j} \\ \dot{u}_{1_k}\end{bmatrix}= \left(\frac{l_e G_3}{2G_1}\right)Gr\theta\begin{bmatrix} 1 \\ 1\end{bmatrix}-\left(\frac{l_e G_4}{6G_1}\right)M\begin{bmatrix} 2 & 1 \\ 1 & 2\end{bmatrix}\begin{bmatrix} u_{1_j} \\ u_{1_k}\end{bmatrix} \tag{30}$$

where a dot denotes differentiation with respect to time. Assembling the element equations for two consecutive elements $y_{i-1} \le y \le y_i$ and $y_i \le y \le y_{i+1}$, we derive

$$\left(\frac{G_2}{G_1 l_e^2}\right)\begin{bmatrix} 1 & -1 & 0 \\ -1 & 2 & -1 \\ 0 & -1 & 1\end{bmatrix}\begin{bmatrix} u_{1_{i-1}} \\ u_{1_i} \\ u_{1_{i+1}}\end{bmatrix}-\left(\frac{\lambda}{2}\right)\begin{bmatrix} 1 & -1 & 0 \\ -1 & 0 & -1 \\ 0 & -1 & 1\end{bmatrix}\begin{bmatrix} u_{1_{i-1}} \\ u_{1_i} \\ u_{1_{i+1}}\end{bmatrix}+\left(\frac{1}{6}\right)\begin{bmatrix} 2 & 1 & 0 \\ 1 & 4 & 1 \\ 0 & 1 & 2\end{bmatrix}\begin{bmatrix} \dot{u}_{1_{i-1}} \\ \dot{u}_{1_i} \\ \dot{u}_{1_{i+1}}\end{bmatrix}= \left(\frac{G_3}{2G_1}\right)Gr\theta\begin{bmatrix} 1 \\ 2 \\ 1\end{bmatrix}-\left(\frac{G_4}{2G_1}\right)M\begin{bmatrix} 2 & 1 & 0 \\ 1 & 4 & 1 \\ 0 & 1 & 2\end{bmatrix}\begin{bmatrix} u_{1_{i-1}} \\ u_{1_i} \\ u_{1_{i+1}}\end{bmatrix} \tag{31}$$

Then putting the members of the row, corresponding to the node equal to zero, we obtain from Eq. (31) where l_e=h

$$\left(\frac{G_2}{G_1 h^2}\right)\left[-u_{1_{i-1}}+2u_{1_i}-u_{1_{i+1}}\right]-\left(\frac{\lambda}{2h}\right)\left[-u_{1_{i-1}}+u_{1_{i+1}}\right]+\left(\frac{1}{6}\right)\left(\dot{u}_{1_{i-1}}+4\dot{u}_{1_i}+\dot{u}_{1_{i+1}}\right)= \frac{G_3 Gr\theta}{G_1}-\frac{G_4 M}{6G_1}\left(u_{1_{i-1}}+4u_{1_i}+u_{1_{i+1}}\right) \tag{32}$$

$$\dot{u}_{1_{i-1}} + 4\dot{u}_{1_i} + \dot{u}_{1_{i+1}} = u_{1_{i-1}}\left[-\frac{G_4 M}{G_1} - \frac{3\lambda}{h} + \frac{6G_2}{G_1 h^2}\right] + u_{1_i}\left[-\frac{4G_4 M}{G_1} - \frac{12G_2}{G_1 h^2}\right] + u_{1_{i+1}}\left[-\frac{G_4 M}{G_1} + \frac{3\lambda}{h} + \frac{6G_2}{G_1 h^2}\right] + \frac{6G_3 Gr\theta}{G_1} \tag{33}$$

Using α -family of time marching schemes (Trapezoidal rule), we have

$$\dot{u}_{1_{i-1}}^{j+1} + 4\dot{u}_{1_i}^{j+1} + \dot{u}_{1_{i+1}}^{j+1} = \left(\frac{2}{k}\right)\left[u_{1_{i-1}}^{j+1} - u_{1_{i-1}}^{j} + 4u_{1_i}^{j+1} - 4u_{1i}^{j} + u_{1_{i+1}}^{j+1} - u_{1_{i+1}}^{j}\right] - \left[\dot{u}_{1_{i-1}}^{j} + 4\dot{u}_{1_i}^{j} + \dot{u}_{1_{i+1}}^{j}\right] \tag{34}$$

Using Eq. (34) at stations j and j+1 in Eq. (35), we get

$$\begin{aligned} &u_{1_{i-1}}^{j+1}\left[\frac{6G_2}{G_1 h^2} - \frac{3\lambda}{h} - \frac{G_4 M}{G_1} - \frac{2}{k}\right] + u_{1_i}^{j+1}\left[-\frac{12G_2}{G_1 h^2} - \frac{4G_4 M}{G_1} - \frac{8}{k}\right] + u_{1_{i+1}}^{j+1}\left[\frac{6G_2}{G_1 h^2} + \frac{3\lambda}{h} - \frac{G_4 M}{G_1} - \frac{2}{k}\right] = \\ &u_{1_{i-1}}^{j}\left[-\frac{6G_2}{G_1 h^2} + \frac{G_4 M}{G_1} + \frac{3\lambda}{h} - \frac{2}{k}\right] + u_{1_i}^{j}\left[\frac{12G_2}{G_1 h^2} + \frac{4G_4 M}{G_1} - \frac{8}{k}\right] + u_{1_{i+1}}^{j}\left[-\frac{6G_2}{G_1 h^2} - \frac{3\lambda}{h} + \frac{G_4 M}{G_1} - \frac{2}{k}\right] - \frac{6G_3 Gr\theta}{G_1}\left[T_i^j + T_i^{j+1}\right] \end{aligned} \tag{35}$$

By Crank Nicolson Method, we have $T_i^j + T_i^{j+1} = T_i^j$.

The given system of Eq. (35) is converted into Matrix Tridiagonal form AX=B. Aloft equations are scrutinized for the numerical solutions of velocity and temperature stencils via Thomas algorithm [55]. The time and spatial step sizes Δt = 0.01, Δy = 0.2 along t and y directions are selected to give accurate results. A 'δ' mesh sensitivity analysis with slightly revised values of the mesh distance in the t – and y – directions, i.e. k and h, has been operated through MATLAB program to define an optimal mesh system for u_1, θ. Also, we performed grid independent analysis for various grid sizes 81x151, 161x301, 321x601 which is pointed in Figure 3 and confirmed to be in excellent agreement. Hence, we achieved mesh independence for solutions with excellent stability and convergence. To confirm the exactitude of the ciphered data, the temperature stencils of the current work in the absence of convective, and viscous dissipation terms when δ_2 = 0 are compared with the analytical relation given by Eq. (15) in Figure 4. This authorizes the present ciphered technique is apt for the current simulation.

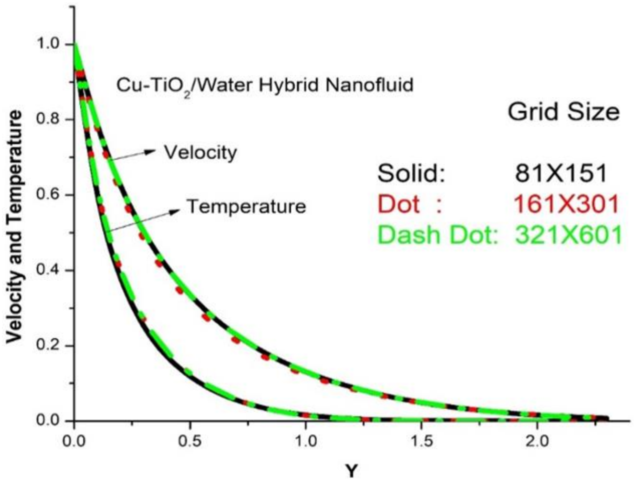

Fig. 3. Grid independence test

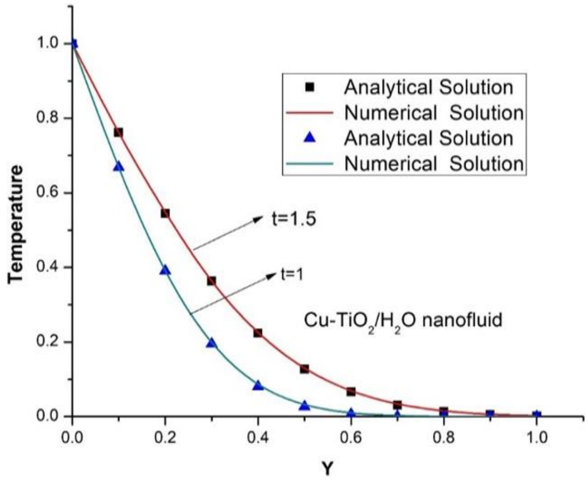

Fig. 4. Comparison of numerical and analytical solution

5. Result Analysis

The pronouncement of this segment is to examine the corollary of numerous ambient flow parameters such as Gr, M, N, Ec, ωt , t, δ_2 , λ , Nu, C_f, and these are presented through tables and pictorial representation. In current scrutiny, consider P_r = 6.2, M=5, Ec=0.09, N = 2, Gr = 10, $\lambda = 0.2$, t = 0.5, $\omega t = \pi / 3$, δ_1 = 0.05, δ_2 = 0.05, and n_1 = 3 (spherical shaped nanoparticles) unless otherwise defined. From a chemical engineering and thermodynamic perspective, the Grashof number provides understanding the interaction between buoyant and viscous forces in natural convection circumstances. An increase in Grashof number signifies dominance in buoyant forces causes inclination for fluid motion and thus momentum elevates, and thermal stencil decelerates, as exposed in Figure 5 and Figure 6. As velocity booms with Gr, the skin friction coefficient for hybrid nano liquid escalates and is lower than that of nano liquid, as displayed in Table 4. Table 3 also perceived that the heat transfer rate with hybrid nano liquid is more than that corresponding to a regular nano liquid with similar constraints and that it amplifies as Gr rises.

Table 3
Nusselt number values for Pr = 6.2

Gr	λ	Ec	N	M	ωt	t	δ_2	Nusselt Number	
								Cu-H_2O	Cu-TiO_2-H_2O
5	0.2	0.09	2	5	π /3	1.5	0.05	2.2535	2.3084
10	0.2	0.09	2	5	π /3	1.5	0.05	2.3132	2.3778
15	0.2	0.09	2	5	π /3	1.5	0.05	2.3519	2.4276
5	0.4	0.09	2	5	π /3	1.5	0.05	3.1175	3.1854
5	0.6	0.09	2	5	π /3	1.5	0.05	4.0632	4.1307
5	0.2	0.09	3	5	π /3	1.5	0.05	2.4419	2.4963
5	0.2	0.09	4	5	π /3	1.5	0.05	2.5143	2.5622
5	0.2	0.09	2	6	π /3	1.5	0.05	2.3003	2.3632
5	0.2	0.09	2	7	π /3	1.5	0.05	2.2932	2.3561
5	0.2	0.09	2	5	π /6	1.5	0.05	2.9725	3.0723
5	0.2	0.09	2	5	π /2	1.5	0.05	1.4044	1.4214
5	0.2	0.08	2	5	π /3	1.5	0.05	2.3467	2.4178
5	0.2	0.07	2	5	π /3	1.5	0.05	2.3804	2.4579
5	0.2	0.09	2	5	π /3	0.5	0.05	3.5626	3.7156
5	0.2	0.09	2	5	π /3	1	0.05	2.6906	2.7822
5	0.2	0.09	2	5	π /3	1	0.10	2.2646	2.3226
5	0.2	0.09	2	5	π /3	1	0.15	2.3251	2.3824

Table 4
Skin Friction Coefficient Values for Pr = 6.2

Gr	λ	Ec	N	M	ωt	t	δ_2	Skin Friction Coefficient	
								Cu-H_2O	Cu-TiO_2-H_2O
5	0.2	0.09	2	5	π /3	1.5	0.05	-4.0506	-4.3461
10	0.2	0.09	2	5	π /3	1.5	0.05	-2.5864	-2.7344
15	0.2	0.09	2	5	π /3	1.5	0.05	-0.8170	-1.4135
5	0.4	0.09	2	5	π /3	1.5	0.05	-3.2369	-3.2394
5	0.6	0.09	2	5	π /3	1.5	0.05	-3.9978	-3.8199
5	0.2	0.09	3	5	π /3	1.5	0.05	-2.6449	-2.7719
5	0.2	0.09	4	5	π /3	1.5	0.05	-2.6772	-2.7924
5	0.2	0.09	2	6	π /3	15	0.05	-3.3365	-3.3735
5	0.2	0.09	2	7	π /3	1.5	0.05	-4.0041	-3.9429
5	0.2	0.09	2	5	π /6	1.5	0.05	-1.7440	-2.1050
5	0.2	0.09	2	5	π /2	1.5	0.05	-3.7352	-3.5930
5	0.2	0.08	2	5	π /3	1.5	0.05	-2.5949	-2.7408
5	0.2	0.07	2	5	π /3	1.5	0.05	-2.6035	-2.7473
5	0.2	0.09	2	5	π /3	0.5	0.05	-3.3454	-3.4617
5	0.2	0.09	2	5	π /3	1	0.05	-2.8421	-2.9109
5	0.2	0.09	2	5	π /3	1	0.10	-4.1290	-4.4213
5	0.2	0.09	2	5	π /3	1	0.15	-4.1326	-4.4341

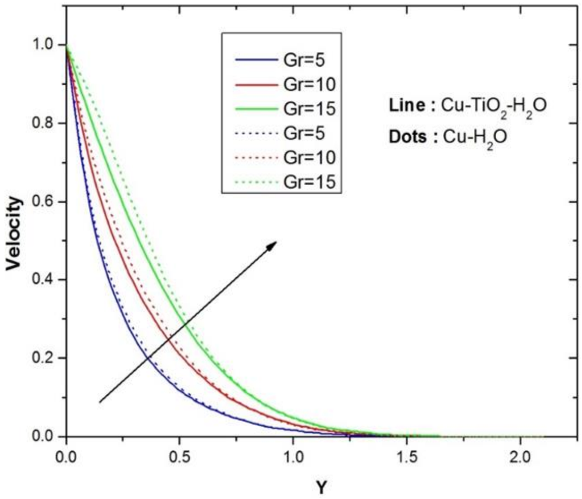

Fig. 5. Collation of Gr on Velocity pattern

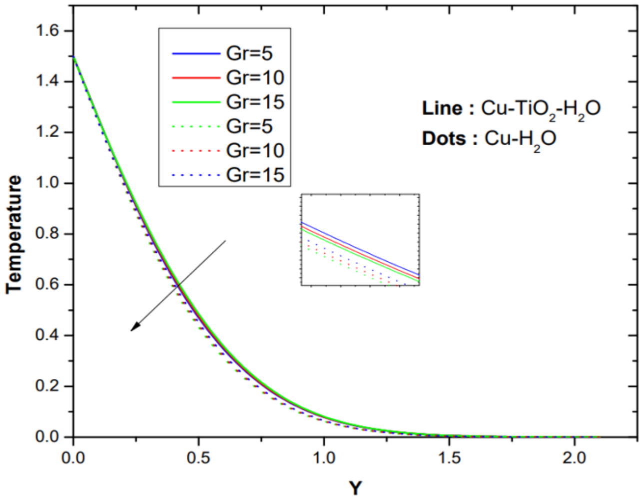

Fig. 6. Collation of Gr on Temperature pattern

Figure 7 and Figure 8 potray's the enhancement in velocity and temperature as Eckert number enhances. This is real, because enhancement in Eckert number produces more heat in between liquid particles due to frictional forces. Table 3 points out that due to supersize of Ec, the Nusselt number is larger in hybrid nano liquids in contrast to nano liquids. From Table 4 it is clear that skin friction coefficient enlarges for both liquids due to the Ec amplification, which can have conclusion for mixing, heat transfer, and energy efficiency in several chemical engineering and thermodynamic processes. It can be seen from Figure 9 and Figure 10 that enlargement in suction parameter, decelerates the velocity and temperature of both liquids. Physically, it is a fact that on employing suction on the plate surface, catalyses the liquid into the plane, as a result curtailment of momentum and thermal boundary layers lowered as λ rises. In chemical engineering and thermodynamics processes, this tends to reduce fluid velocities, alter temperature profiles, and influence mixing and thermal transfer effectiveness. The Nusselt number elevates upon the escalation of λ for both type of liquids and jacked up in hybrid nano liquids in contrast to nano liquids, which is obeyed from Table 3. The dwindling of coefficient of skin friction with enlargement of λ for both the liquids is pointed in Table 4 and also it is tipped that the hybrid nano liquids coefficient of skin friction is less than that of regular nano liquids.

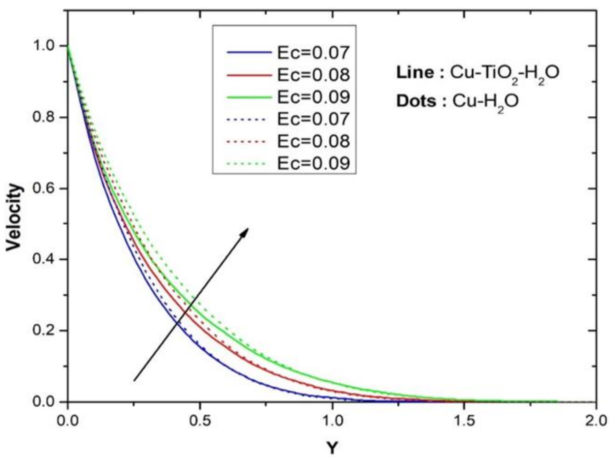

Fig. 7. Collation of Ec on Velocity pattern

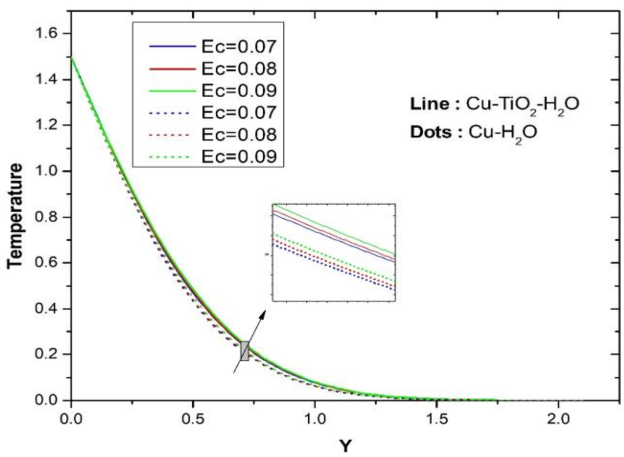

Fig. 8. Collation of Ec on Temperature pattern

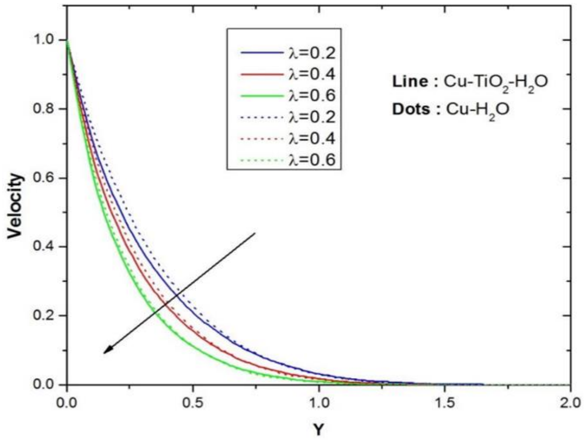

Fig. 9. Collation of λ on Velocity pattern

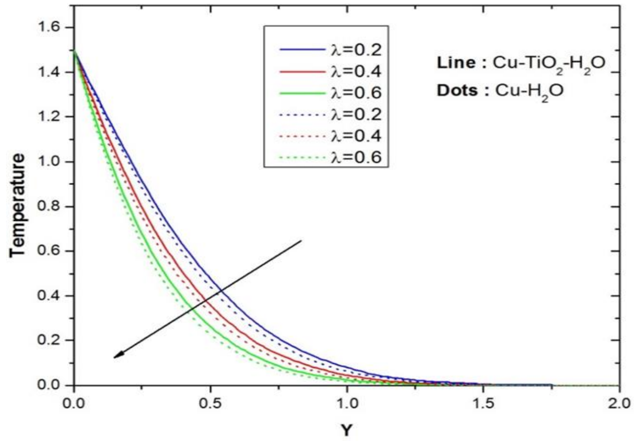

Fig. 10. Collation of λ on Temperature pattern

From Figure 11 and 12, the velocity of both hybrid nano liquids and nano liquids decreases as M grows whereas temperature increases for both liquids. From chemical engineering and thermodynamic perspective, upwind in M yields in piling up the Lorentz force which catalyzes opposing circulation of fluid, results in development of stress, as a result temperature builds up. It is documented in Table 3 that proliferation of M, yields in depletion of Nusselt number for both type of liquids, the Nusselt number in hybrid nano liquids dominates over nano liquids. From the Table 4, it is noted that due to amplification of M, drop in skin friction is confirmed. However, the skin friction of hybrid nano liquid is lesser than that of nano liquid. From Figure 13 and Figure 14 we understood that due to the amplification of N both velocity and temperature features shrinks. Physically we agree that thermal radiation N is a function of ratio between conduction to radiation, as N accentuates, which results in the lessening of radiative flux induces the suppression of energy transport to the liquid causing the cooling and thinning of momentum and thermal boundary layers from the aspect of chemical engineering and thermodynamics.

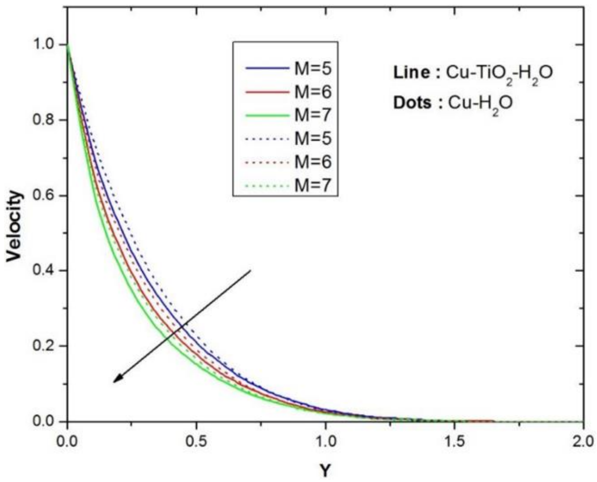

Fig. 11. Collation of M on Velocity pattern

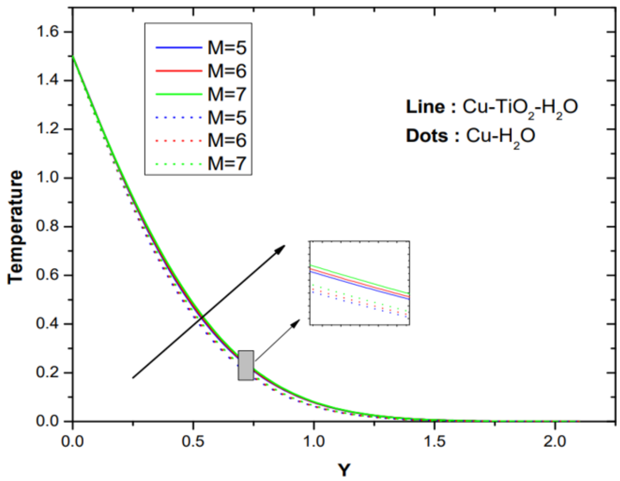

Fig. 12. Collation of M on Temperature pattern

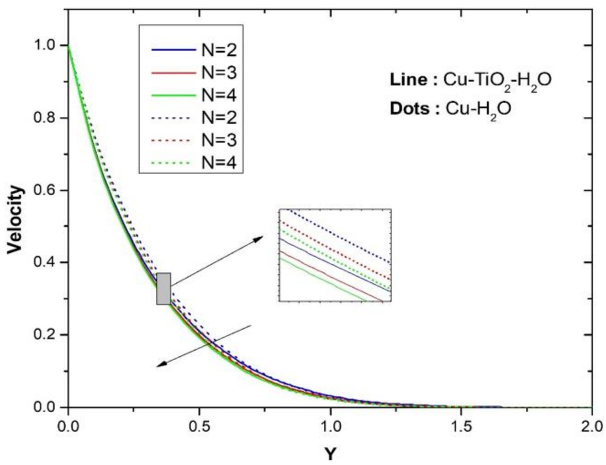

Fig. 13. Collation of N on Velocity pattern

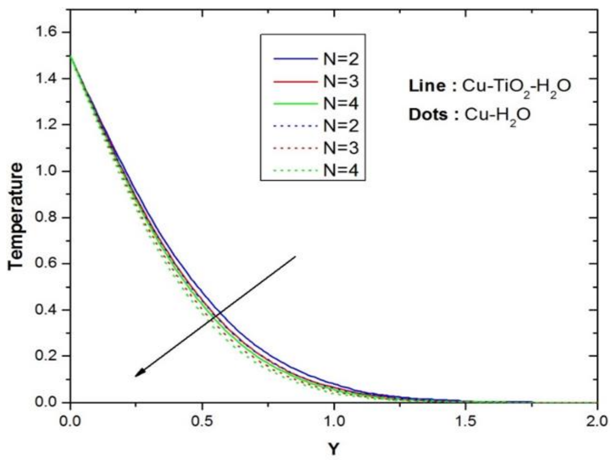

Fig. 14. Collation of N on Temperature pattern

Figure 15 and Figure 16 points that each of two hybrid nano liquids and nano liquids velocity drops, but the temperature accelerates with the expansion of δ_2. Since appending of further nanoparticles leads to ease off the flow area and employ excess energy, which intensify the temperature and hence condense thermal boundary layer by chemical engineering and thermodynamics aspects. Intensification of δ_2 slows down the velocity stream, which evidently drops both types of nano liquids skin friction, shown in Table 4. Figure 17 and Figure 18 narrates that as t escalates the velocity and temperature together enlarges for both the liquids. Also, with the hike in t Nusselt number boosts up for both type of liquids and the Nusselt number is larger in Hybrid nano liquids in contrast to nano liquids which is spotted in Table 3 whereas the revert trend is pointed out for skin friction coefficient which is highlighted in Table 4. Proliferation of ωt leads to downsize of velocity and temperature together for both the nano liquids as seen in Figure 19 and Figure 20. Upon the rise in ωt, Nusselt number reduces for both type of liquids, Nusselt number is large in Hybrid nano liquids in contrast to nano liquids. It is noted in Table 4 that as ωt rises, both liquids skin friction coefficient drops.

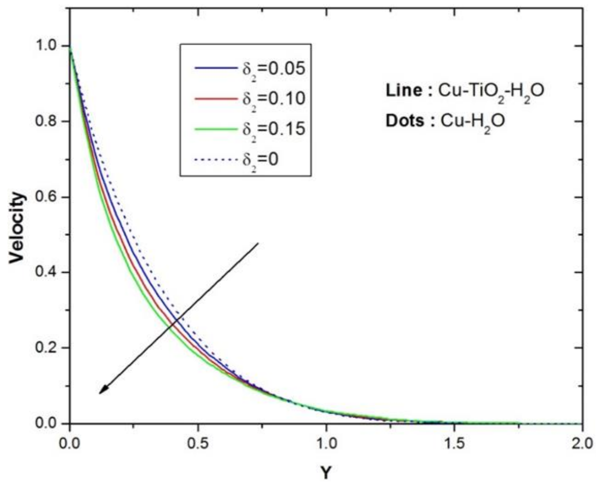

Fig. 15. Collation of δ_2 on Velocity pattern

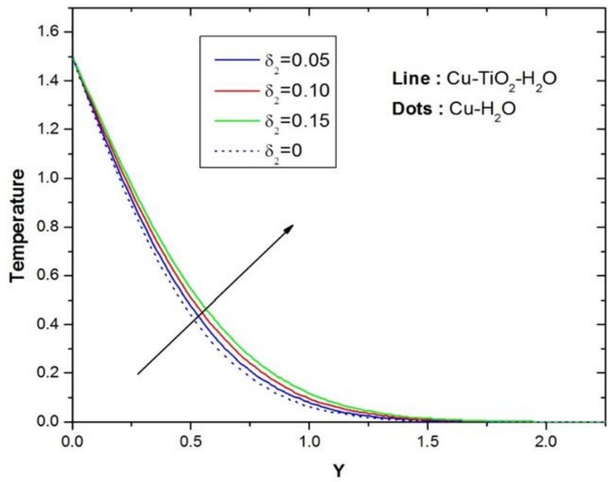

Fig. 16. Collation of δ_2 on Velocity pattern

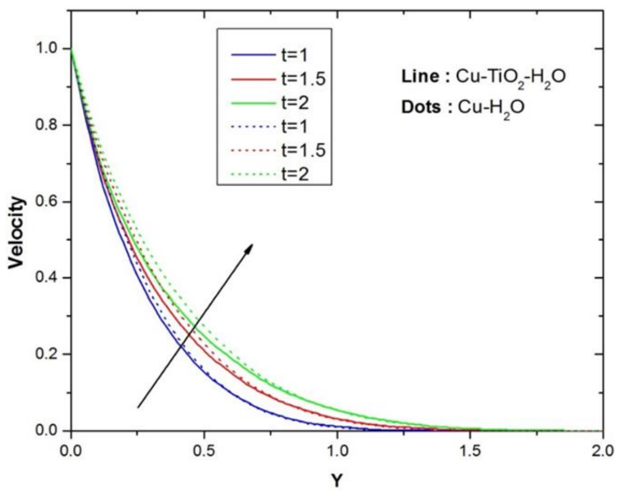

Fig. 17. Collation of t on Velocity pattern

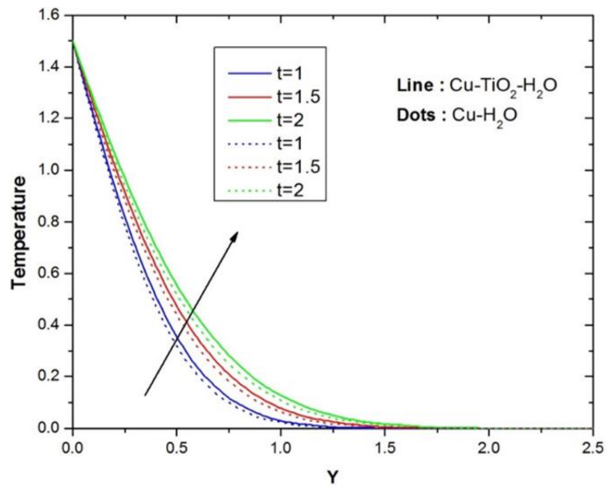

Fig. 18. Collation of t on Temperature pattern

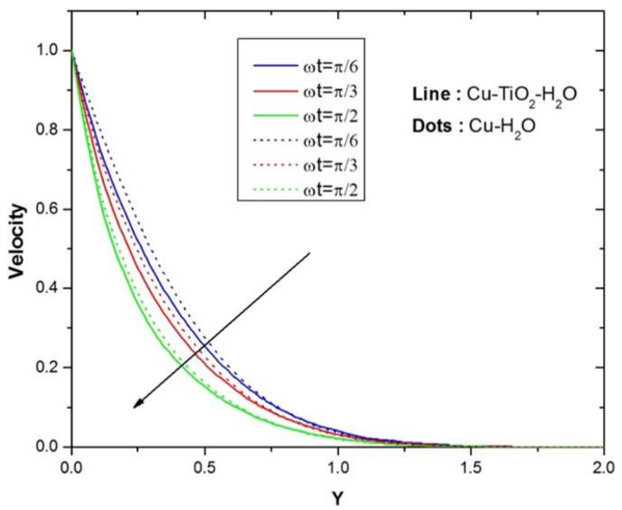

Fig. 18. Collation of ωt on Velocity pattern

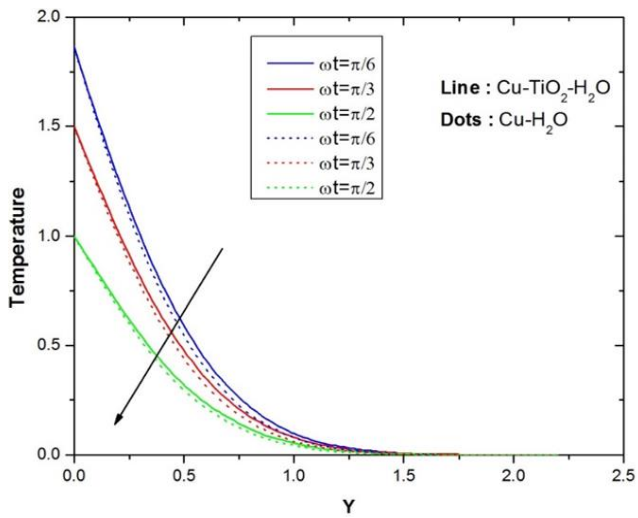

Fig. 19. Collation of ωt on Temperature pattern

6. Conclusions

The outcomes of the present analysis:

i. Superior heat transmission through Cu-TiO_2 - H_2O can be attained than Cu- H_2O by choosing Cu-TiO_2 - H_2O as a working liquid.

ii. The lesser skin friction coefficient is celebrated for Cu-TiO_2 - H_2O than Cu-H_2O. Velocity, skin friction parameters are spotted to increase with Gr. However, temperature and Nusselt numbers remain constant for both liquid cases. As Gr enhances, upsurge in buoyancy takes place, as a consequence upswing in velocity is recorded.

iii. Velocity, temperature and skin friction parameters are shrinking functions of λ for both liquid cases. However, Nusselt number is an inclining function of λ. Physically, it is a fact that on employing suction on the plate surface, catalyzes the liquid into the plane, as a result curtailment of momentum and thermal boundary layers lowered as λ rises.

iv. Velocity is spotted to reduce with ωt, but skin friction is spotted to grow with ωt. However, temperature and Nusselt numbers remain constant for two types of liquids.

v. Velocity and temperature are declining functions of N for nano liquid and hybrid nano liquid. However, Nusselt number inclines with N, but skin friction declines with N. Physically we agree that thermal radiation N is relation between conduction to radiation, as N accentuates, which outcomes the lessening of radiative flux induces the suppression of energy transport to the fluid causing the cooling and thinning of momentum and thermal boundary layers.

vi. There is enhancement in velocity and temperature as Eckert number enhances. It is fact, because enhancement in Eckert number produces more heat in between liquid particles due to frictional forces.

vii. Due to supersize of Ec, the Nusselt number is larger in hybrid nano liquids in contrast to nano liquids. Skin friction coefficient enlarges for both liquids due to the Ec amplification, which can have conclusion for mixing, heat transfer, and energy efficiency in several chemical engineering and thermodynamic processes.

viii. The velocity of both hybrid nano liquids and nano liquids decreases as M grows whereas temperature increases for both liquids. From chemical engineering and thermodynamic perspective, upwind in M yields in piling up the Lorentz force which catalyzes opposing circulation of fluid, results in development of stress, as a result temperature builds up.

ix. Velocity is spotted to reduce with δ_2, but the temperature is spotted to grow with δ_2 for both liquid cases. Velocity, temperature and skin friction parameters are inclining functions of time t for both liquids. However, Nusselt number is the declining function of time t.

x. Some of the applications of the current model which are efficiently used in different engineering fields including hydromagnetic motion in geothermal reservoirs, nuclear coolants, MHD power generation, thermal imaging cameras like building inspections, earth's climate systems such as global temperatures, heat exchanger design where the efficiency of heat transfer between the fluids is designed etc.

Acknowledgement
This study is supported via funding from Prince Sattam bin Abdulaziz University, Alkharj Saudi Arabia, project number (PSAU/2023/R/1444). First author would like to thank KLEF for providing fulltime fellowship for research work and we are also grateful to Editors and Reviewers for their valuable suggestions.

References

[1] Vempati, S. R., and A. B. Laxmi-Narayana-Gari. "Soret and Dufour effects on unsteady MHD flow past an infinite vertical porous plate with thermal radiation." *Applied Mathematics and Mechanics* 31 (2010): 1481-1496. https://doi.org/10.1007/s10483-010-1378-9

[2] Rashidi, Mohammad Mehdi, Behnam Rostami, Navid Freidoonimehr, and Saeid Abbasbandy. "Free convective heat and mass transfer for MHD fluid flow over a permeable vertical stretching sheet in the presence of the radiation and buoyancy effects." *Ain Shams Engineering Journal* 5, no. 3 (2014): 901-912. https://doi.org/10.1016/j.asej.2014.02.007

[3] Daniel, Yahaya Shagaiya, and Simon K. Daniel. "Effects of buoyancy and thermal radiation on MHD flow over a stretching porous sheet using homotopy analysis method." *Alexandria Engineering Journal* 54, no. 3 (2015): 705-712. https://doi.org/10.1016/j.aej.2015.03.029

[4] Singh, Jitendra Kumar, Gauri Shenker Seth, and Saikh Ghousia Begum. "Unsteady MHD natural convection flow of a rotating viscoelastic fluid over an infinite vertical porous plate due to oscillating free-stream." *Multidiscipline Modeling in Materials and Structures* 14, no. 2 (2017): 236-260. https://doi.org/10.1108/MMMS-06-2017-0054

[5] Rajesh, V., A. J. Chamkha, Ch Sridevi, and A. F. Al-Mudhaf. "A numerical investigation of transient MHD free convective flow of a nanofluid over a moving semi-infinite vertical cylinder." *Engineering Computations* 34, no. 5 (2017): 1393-1412. https://doi.org/10.1108/EC-03-2016-0090

[6] Singh, J. K., N. Joshi, and P. Rohidas. "Unsteady MHD natural convective flow of a rotating Walters'-B fluid over an oscillating plate with fluctuating wall temperature and concentration." *Journal of Mechanics* 34, no. 4 (2018): 519-532. https://doi.org/10.1017/jmech.2017.25

[7] Chamkha, Ali J., A. S. Dogonchi, and D. D. Ganji. "Magneto-hydrodynamic flow and heat transfer of a hybrid nanofluid in a rotating system among two surfaces in the presence of thermal radiation and Joule heating." *AIP Advances* 9, no. 2 (2019). https://doi.org/10.1063/1.5086247

[8] Kumar, P. Pramod, B. Shankar Goud, and Bala Siddulu Malga. "Finite element study of Soret number effects on MHD flow of Jeffrey fluid through a vertical permeable moving plate." *Partial Differential Equations in Applied Mathematics* 1 (2020): 100005. https://doi.org/10.1016/j.padiff.2020.100005

[9] Khan, Dolat, Arshad Khan, Ilyas Khan, Farhad Ali, Faizan ul Karim, and I. Tlili. "Effects of relative magnetic field, chemical reaction, heat generation and Newtonian heating on convection flow of Casson fluid over a moving vertical plate embedded in a porous medium." *Scientific Reports* 9, no. 1 (2019): 400. https://doi.org/10.1038/s41598-018-36243-0

[10] Ali, Farhad, Muhammad Bilal, Madeha Gohar, Ilyas Khan, Nadeem Ahmad Sheikh, and Kottakkaran Sooppy Nisar. "A report on fluctuating free convection flow of heat absorbing viscoelastic dusty fluid past in a horizontal channel with MHD effect." *Scientific Reports* 10, no. 1 (2020): 8523. https://doi.org/10.1038/s41598-020-65252-1

[11] Kavitha, M., V. Rajesh, M. P. Mallesh, and Ali J. Chamka. "Unsteady CNTs kerosene nanofluid flow past a vertical plate with heat transfer under the influence of thermal radiation." In *AIP Conference Proceedings*, vol. 2246, no. 1. AIP Publishing, 2020. https://doi.org/10.1063/5.0014577

[12] Mallesh, M. P., V. Rajesh, M. Kavitha, and Ali J. Chamkha. "Study of time dependent free convective kerosene-nanofluid flow with viscous dissipation past a porous plate." In *AIP Conference Proceedings*, vol. 2246, no. 1. AIP Publishing, 2020. https://doi.org/10.1063/5.0014451

[13] Ali, Aamir, A. Noreen, S. Saleem, A. F. Aljohani, and M. Awais. "Heat transfer analysis of Cu-Al_2O_3 hybrid nanofluid with heat flux and viscous dissipation." *Journal of Thermal Analysis and Calorimetry* 143, no. 3 (2021): 2367-2377. https://doi.org/10.1007/s10973-020-09910-6

[14] Goud, B. Shankar. "Heat generation/absorption influence on steady stretched permeable surface on MHD flow of a micropolar fluid through a porous medium in the presence of variable suction/injection." *International Journal of Thermofluids* 7 (2020): 100044. https://doi.org/10.1016/j.ijft.2020.100044

[15] Vemula, Rajesh, M. Kavitha, and Mikhail A. Sheremet. "Effects of internal heat generation and Lorentz force on unsteady hybrid nanoliquid flow and heat transfer along a moving plate with nonuniform temperature." *Heat Transfer* 50, no. 3 (2021): 2975-2996. https://doi.org/10.1002/htj.22014

[16] Singh, Jitendra Kumar, Suneetha Kolasani, and Vishwanath Savanur. "Significance of Hall effect on heat and mass transport of titanium alloy-water-based nanofluid flow past a vertical surface with IMF effect." *Heat Transfer* 50, no. 6 (2021): 5793-5812. https://doi.org/10.1002/htj.22149

[17] Singh, Jitendra Kumar, Suneetha Kolasani, and G. S. Seth. "Heat and mass transport nature of MHD nanofluid flow over a magnetized and convectively heated surface including Hall current, magneto and thermo diffusions impacts." *Ricerche di Matematica* (2022): 1-21. https://doi.org/10.1007/s11587-022-00687-4

[18] Sharma, B. K., and Rishu Gandhi. "Combined effects of Joule heating and non-uniform heat source/sink on unsteady MHD mixed convective flow over a vertical stretching surface embedded in a Darcy-Forchheimer porous medium." *Propulsion and Power Research* 11, no. 2 (2022): 276-292. https://doi.org/10.1016/j.jppr.2022.06.001

[19] Sharma, B. K., Anup Kumar, Rishu Gandhi, and M. M. Bhatti. "Exponential space and thermal-dependent heat source effects on electro-magneto-hydrodynamic Jeffrey fluid flow over a vertical stretching surface." *International Journal of Modern Physics B* 36, no. 30 (2022): 2250220. https://doi.org/10.1142/S0217979222502204

[20] Kumar, Anup, Bhupendra K. Sharma, Rishu Gandhi, Nidhish K. Mishra, and M. M. Bhatti. "Response surface optimization for the electromagnetohydrodynamic Cu-polyvinyl alcohol/water Jeffrey nanofluid flow with an exponential heat source." *Journal of Magnetism and Magnetic Materials* 576 (2023): 170751. https://doi.org/10.1016/j.jmmm.2023.170751

[21] Sharma, Bhupendra Kumar, Anup Kumar, Rishu Gandhi, Muhammad Mubashir Bhatti, and Nidhish Kumar Mishra. "Entropy generation and thermal radiation analysis of EMHD Jeffrey nanofluid flow: Applications in solar energy." *Nanomaterials* 13, no. 3 (2023): 544. https://doi.org/10.3390/nano13030544

[22] Gandhi, Rishu, Bhupendra Kumar Sharma, Nidhish Kumar Mishra, and Qasem M. Al-Mdallal. "Computer Simulations of EMHD Casson Nanofluid Flow of Blood through an Irregular Stenotic Permeable Artery: Application of Koo-Kleinstreuer-Li Correlations." *Nanomaterials* 13, no. 4 (2023): 652. https://doi.org/10.3390/nano13040652

[23] Reddy, Y. Dharmendar, B. Shankar Goud, Kottakkaran Sooppy Nisar, B. Alshahrani, Mona Mahmoud, and Choonkil Park. "Heat absorption/generation effect on MHD heat transfer fluid flow along a stretching cylinder with a porous medium." *Alexandria Engineering Journal* 64 (2023): 659-666. https://doi.org/10.1016/j.aej.2022.08.049

[24] Vemula, Rajesh, Ali J. Chamkha, and Mallesh M. P. "Nanofluid flow past an impulsively started vertical plate with variable surface temperature." *International Journal of Numerical Methods for Heat & Fluid Flow* 26, no. 1 (2016): 328-347. https://doi.org/10.1108/HFF-07-2014-0209

[25] Devi, S. P. Anjali, and S. Suriya Uma Devi. "Numerical investigation of hydromagnetic hybrid Cu-Al_2O_3/water nanofluid flow over a permeable stretching sheet with suction." *International Journal of Nonlinear Sciences and Numerical Simulation* 17, no. 5 (2016): 249-257. https://doi.org/10.1515/ijnsns-2016-0037

[26] Devi, S. Suriya Uma, and S. P. Anjali Devi. "Numerical investigation of three-dimensional hybrid Cu-Al_2O_3/water nanofluid flow over a stretching sheet with effecting Lorentz force subject to Newtonian heating." *Canadian Journal of Physics* 94, no. 5 (2016): 490-496. https://doi.org/10.1139/cjp-2015-0799

[27] Bodduna, Jamuna, M. P. Mallesh, Chandra Shekar Balla, and Sabir Ali Shehzad. "Activation energy process in bioconvection nanofluid flow through porous cavity." *Journal of Porous Media* 25, no. 4 (2022). https://doi.org/10.1615/JPorMedia.2022040230

[28] Asogwa, Kanayo Kenneth, B. Shankar Goud, Nehad Ali Shah, and Se-Jin Yook. "Rheology of electromagnetohydrodynamic tangent hyperbolic nanofluid over a stretching riga surface featuring dufour effect and activation energy." *Scientific Reports* 12, no. 1 (2022): 14602. https://doi.org/10.1038/s41598-022-18998-9

[29] Rajesh, V., M. Kavitha, and M. P. Mallesh. "Effects of MHD and Thermal Radiation on Unsteady Free Convective Flow of a Hybrid Nanofluid Past a Vertical Plate." In *International Conference on Applied Analysis, Computation and Mathematical Modelling in Engineering*, pp. 21-41. Singapore: Springer Nature Singapore, 2021. https://doi.org/10.1007/978-981-19-1824-7_2

[30] Sharma, Bhupendra K., Parikshit Sharma, Nidhish K. Mishra, and Unai Fernandez-Gamiz. "Darcy-Forchheimer hybrid nanofluid flow over the rotating Riga disk in the presence of chemical reaction: Artificial neural network approach." *Alexandria Engineering Journal* 76 (2023): 101-130. https://doi.org/10.1016/j.aej.2023.06.014

[31] Mallesh, M. P., Oluwole D. Makinde, Rajesh Vemula, and M. Kavitha. "Time-dependent thermal circulation of hybrid nano liquid past an oscillating porous plate with heat generation and thermal radiation." *Journal of Applied Nonlinear Dynamics* 12, no. 1 (2023): 171-189. https://doi.org/:10.5890/JAND.2023.03.012

[32] Reddy, B. Prabhakar. "Radiation and chemical reaction effects on unsteady MHD free convection parabolic flow past an infinite isothermal vertical plate with viscous dissipation." *International Journal of Applied Mechanics and Engineering* 24, no. 2 (2019): 343-358. https://doi.org/10.2478/ijame-2019-0022

[33] Zainal, N. A., Roslinda Nazar, Kohilavani Naganthran, and Ioan Pop. "Viscous dissipation and MHD hybrid nanofluid flow towards an exponentially stretching/shrinking surface." *Neural Computing and Applications* (2021): 1-11. https://doi.org/10.1007/s00521-020-05645-5

[34] Bestman, A. R., and S. K. Adjepong. "Unsteady hydromagnetic free-convection flow with radiative heat transfer in a rotating fluid: I. Incompressible optically thin fluid." *Astrophysics and Space Science* 143 (1988): 73-80. https://doi.org/10.1007/BF00636756

[35] Makinde, Oluwole Daniel, and A. Ogulu. "The effect of thermal radiation on the heat and mass transfer flow of a variable viscosity fluid past a vertical porous plate permeated by a transverse magnetic field." *Chemical Engineering Communications* 195, no. 12 (2008): 1575-1584. https://doi.org/10.1080/00986440802115549

[36] Pal, Dulal, and Hiranmoy Mondal. "Radiation effects on combined convection over a vertical flat plate embedded in a porous medium of variable porosity." *Meccanica* 44 (2009): 133-144. https://doi.org/10.1007/s11012-008-9156-0

[37] Jat, R. N., and Santosh Chaudhary. "Radiation effects on the MHD flow near the stagnation point of a stretching sheet." *Zeitschrift für angewandte Mathematik und Physik* 61 (2010): 1151-1154. https://doi.org/10.1007/s00033-010-0072-5

[38] Sandeep, N., C. Sulochana, and B. Rushi Kumar. "Unsteady MHD radiative flow and heat transfer of a dusty nanofluid over an exponentially stretching surface." *Engineering Science and Technology, an International Journal* 19, no. 1 (2016): 227-240. https://doi.org/10.1016/j.jestch.2015.06.004

[39] Chaudhary, Santosh, and Mohan Kumar Choudhary. "Partial slip and thermal radiation effects on hydromagnetic flow over an exponentially stretching surface with suction or blowing." *Thermal Science* 22, no. 2 (2018): 797-808. https://doi.org/10.2298/TSCI160127150C

[40] Kavitha, M., V. Rajesh, and M. P. Mallesh. "Numerical computation of CNTs water based nanofluid flow with heat generation/absorption past an oscillating vertical plate with variable temperature." In *AIP Conference Proceedings*, vol. 2316, no. 1. AIP Publishing, 2021. https://doi.org/10.1063/5.0036442

[41] Vafai, K., and SungJin Kim. "Fluid mechanics of the interface region between a porous medium and a fluid layer-an exact solution." *International Journal of Heat and Fluid Flow* 11, no. 3 (1990): 254-256. https://doi.org/10.1016/0142-727X(90)90045-D

[42] Ishak, Anuar, Roslinda Nazar, Norihan M. Arifin, and Ioan Pop. "Dual solutions in mixed convection flow near a stagnation point on a vertical porous plate." *International Journal of Thermal Sciences* 47, no. 4 (2008): 417-422. https://doi.org/10.1016/j.ijthermalsci.2007.03.005

[43] Rosali, Haliza, Anuar Ishak, and Ioan Pop. "Stagnation point flow and heat transfer over a stretching/shrinking sheet in a porous medium." *International Communications in Heat and Mass Transfer* 38, no. 8 (2011): 1029-1032. https://doi.org/10.1016/j.icheatmasstransfer.2011.04.031

[44] Shit, G. C., R. Haldar, and S. Mandal. "Entropy generation on MHD flow and convective heat transfer in a porous medium of exponentially stretching surface saturated by nanofluids." *Advanced Powder Technology* 28, no. 6 (2017): 1519-1530. https://doi.org/10.1016/j.apt.2017.03.023

[45] Chaudhary, Susheela, Santosh Chaudhary, and Sawai Singh. "Heat Transfer in Hydromagnetic Flow over an Unsteady Stretching Permeable Sheet." *International Journal of Mathematical, Engineering and Management Sciences* 4, no. 4 (2019): 1018. https://doi.org/10.33889/IJMEMS.2019.4.4-081

[46] Chaudhary, Susheela, Santosh Chaudhary, and Mohan Kumar Choudhary. "Numerical investigation of unsteady MHD flow and radiation heat transfer past a stretching surface in porous media with viscous dissipation and heat generation/absorption." *Indian Journal of Pure and Applied Physics* 58, no. 2 (2020): 71-78.

[47] Waini, Iskandar, Anuar Ishak, Teodor Groşan, and Ioan Pop. "Mixed convection of a hybrid nanofluid flow along a vertical surface embedded in a porous medium." *International Communications in Heat and Mass Transfer* 114 (2020): 104565. https://doi.org/10.1016/j.icheatmasstransfer.2020.104565

[48] Sharma, Bhupendra K., Parikshit Sharma, Nidhish K. Mishra, Samad Noeiaghdam, and Unai Fernandez-Gamiz. "Bayesian regularization networks for micropolar ternary hybrid nanofluid flow of blood with homogeneous and heterogeneous reactions: Entropy generation optimization." *Alexandria Engineering Journal* 77 (2023): 127-148. https://doi.org/10.1016/j.aej.2023.06.080

[49] Tiwari, Raj Kamal, and Manab Kumar Das. "Heat transfer augmentation in a two-sided lid-driven differentially heated square cavity utilizing nanofluids." *International Journal of Heat and Mass Transfer* 50, no. 9-10 (2007): 2002-2018. https://doi.org/10.1016/j.ijheatmasstransfer.2006.09.034

[50] Schlichting, Hermann, and Klaus Gersten. *Boundary-layer theory*. Springer, 2001. https://doi.org/10.1007/978-3-642-85829-1

[51] Das, S., R. N. Jana, and O. D. Makinde. "Magnetohydrodynamic free convective flow of nanofluids past an oscillating porous flat plate in a rotating system with thermal radiation and hall effects." *Journal of Mechanics* 32, no. 2 (2016): 197-210. https://doi.org/10.1017/jmech.2015.49

[52] Rajesh, V., and Ali J. Chamkha. "Unsteady convective flow past an exponentially accelerated infinite vertical porous plate with Newtonian heating and viscous dissipation." *International Journal of Numerical Methods for Heat & Fluid Flow* 24, no. 5 (2014): 1109-1123. https://doi.org/10.1108/HFF-05-2012-0122

[53] Reddy, Junuthula Narasimha. *An introduction to the finite element method*. McGraw-Hill Education, 2006.

[54] Bathe, Klaus-Jürgen. *Finite element procedures*. Prentice Hall, 1996.

[55] Carnahan, Brice, H. A. Luther, and James O. Wilkes. *Applied numerical methods*. Wiley, 1969.